

Rainfall characterisation by application of standardised precipitation index (SPI) in Peninsular Malaysia

Fadhilah Yusof · Foo Hui-Mean · Jamaludin Suhaila ·
Zulkifli Yusop · Kong Ching-Yee

Received: 19 June 2012 / Accepted: 23 April 2013 / Published online: 8 May 2013
© Springer-Verlag Wien 2013

Abstract The interpretations of trend behaviour for dry and wet events are analysed in order to verify the dryness and wetness episodes. The fitting distribution of rainfall is computed to classify the dry and wet events by applying the standardised precipitation index (SPI). The rainfall amount for each station is categorised into seven categories, namely extremely wet, severely wet, moderately wet, near normal, moderately dry, severely dry and extremely dry. The computation of the SPI is based on the monsoon periods, which include the northeast monsoon, southwest monsoon and inter-monsoon. The trends of the dry and wet periods were then detected using the Mann–Kendall trend test and the results indicate that the major parts of Peninsular Malaysia are characterised by increasing droughts rather than wet events. The annual trends of drought and wet events of the randomly selected stations from each region also yield similar results. Hence, the northwest and southwest regions are predicted to have a higher probability of drought occurrence during a dry event and not much rain during the wet event. The east and west regions, on the other hand, are going through a significant upward trend that implies lower rainfall during the drought episodes and heavy rainfall during the wet events.

1 Introduction

Precipitation or rainfall is the primary factor which controls the formation and persistence of droughts and floods. A drought is characterised by a deficiency of water supply over an extended period of time, while a flood is an overflow of water that submerges the land. Droughts and floods are extreme events which may adversely affect social, economic, political, cultural and other functions of a region. Therefore, there have been many studies conducted on extreme events, particularly in characterising the events into dry and wet categories (Sirdas and Sen 2001; Deni et al. 2009; Zhang et al. 2009).

Meteorological droughts, defined as a lack of precipitation in a region over a period of time, are the main focus of this paper. The standardised precipitation index (SPI) (e.g. Bordi et al. 2009) is the most commonly used method to reveal a meteorological drought and is also a successful tool in the estimation of the intensity and duration of drought events. The SPI has been widely used to quantify the precipitation deficit in terms of the probability for multiple time scales, which are designed to reflect the impacts of precipitation deficits on different water resources (McKee et al. 1993). SPI is originally calculated for 3-, 6-, 12-, 24- and 48-month time scales. It is a classification system which is normalised so that drier and wetter climates can be represented in the same way (Sirdas and Sen 2001). As such, it can be used to monitor dry as well as wet periods where negative values indicate drought while positive values indicate wet conditions based on a dimensionless index of SPI (Sonmez et al. 2005).

An analysis of rainfall characteristics is an important component in managing water resources with the development of industrialisation as well as rapid growth in the population (Deni et al. 2009). Therefore, it is of scientific and practical merit to better understand the varying characteristics of dryness and wetness for predicting and preventing disasters brought about by extreme events. The trend analysis for dry and wet

F. Yusof · F. Hui-Mean (✉) · J. Suhaila · Z. Yusop · K. Ching-Yee
Department of Mathematics, Faculty of Science,
Universiti Teknologi Malaysia, 81310, Skudai, Johor, Malaysia
e-mail: huimean87@gmail.com

F. Yusof
e-mail: fadhilahy@utm.my

J. Suhaila
e-mail: suhailasj@utm.my

Z. Yusop
e-mail: zulyusop@utm.my

K. Ching-Yee
e-mail: chingyeekong87@gmail.com

spells is an important element for climate change issues. The Intergovernmental Panel on Climate Change has established a series of reports that summarise the observed climate changes and project future changes, which have emphasised that global warming is a serious issue for national and international security due to the wide spectrum of consequences to the resilience of the population support system (health, energy, water and food security), human security (population dislocation and armed conflict) and political continuity (continuity of governance and economic viability) (Department of Defense 2011). The trend characteristics or persistency will contribute to the prediction of future climatic events due to the dependency on extreme weather events such as drought, flood and landslides (Deni et al. 2009). These contributions will be beneficial for dealing with the global warming issue as the trend identification for dry and wet events is helpful in predicting the future drought and flood episodes in order to have an efficient system and planning in mitigating the negative impacts and reducing the global warming influences.

Hence, this study will focus on characterising the rainfall into dry and wet events using SPI in which the percentages of dryness and wetness could also be evaluated. The objectives of this study are: (1) to obtain the best-fitted distribution in representing the rainfall of Peninsular Malaysia; (2) to detect the properties of dry and wet episodes defined by SPI; (3) to determine the percentage of dry and wet events in each state of Peninsular Malaysia; and (4) to verify the trend for dry and wet events.

2 Study region and data

Peninsular Malaysia (100°E–104°E; 1°N–7°N), also known as West Malaysia, covers an area of about 131,598 km² (Fig. 1). The climate is influenced by two monsoons, namely the northeast monsoon from November to February and the southwest monsoon from May to August. Inter-monsoon periods (March to April and September to October) usually bring more rainfall in the central region.

The daily precipitation dataset, which covers the period from November 1975 to October 2008, was obtained from 75 rain gauge stations in Peninsular Malaysia. The data used are considered good quality data with no missing values throughout the 33-year period. The rain gauge locations are categorised into four regions, namely east, southwest, west and northwest according to their geographical coordinates, respectively. The categorisation is based on the significant variation for different elements among these four regions such as the trend effects and the impacts of adjoining wet days (Suhaila and Jemain 2009; Deni et al. 2009). Location of the rain gauge stations can be seen in Fig. 1 and Table 1. The eastern and western regions are separated by the main range (Banjaran Titiwangsa), which runs from the far north to the

south of Peninsular Malaysia. The main range has significant influence on the spatial rainfall pattern by shading more rain on the east coast during the northeast monsoon due to rain shadow effect. Likewise, the southwest monsoon brings more rain on the west coast (Suhaila and Jemain 2009).

3 Methodology

3.1 Types of probability distributions

Fitting of distribution for the rainfall amount is computed on behalf of all stations under study, and three types of distributions are selected in fitting based on the relation for SPI determination. Gamma distribution is generally assumed to be fitted in SPI calculation (McKee et al. 1993), Weibull distribution is identified as the heavy-tailed distribution in precipitation fitting (Yusof and Hui-Mean 2012), while log-normal distribution is verified as the best-fitted distribution for further SPI computation (Zhang et al. 2009).

Gamma distribution is a two-parameter family, with the probability density function (PDF) and cumulative distribution function (CDF) written as follows:

$$f(x; \alpha, \beta) = x^{(\alpha-1)} \frac{e^{-\frac{x}{\beta}}}{\beta^\alpha \Gamma(\alpha)} \quad (1)$$

$$F(x; \alpha, \beta) = \int_0^x f(u; \alpha, \beta) du = \frac{\gamma\left(\alpha, \frac{x}{\beta}\right)}{\Gamma(\alpha)} \quad (2)$$

for $x > 0$ and $\alpha, \beta > 0$ where $\Gamma(\alpha) = \int_0^\infty x^{\alpha-1} e^{-x} dx$ and $\gamma(s, x) = \int_0^x t^{s-1} e^{-t} dt$ is the lower incomplete gamma function, α is the shape parameter, and β is the scale parameter.

Weibull distribution is a continuous probability with the PDF and CDF written as follows:

$$f(x; \alpha, \beta) = \frac{\beta}{\alpha} \left(\frac{x}{\alpha}\right)^{\beta-1} e^{-\left(\frac{x}{\alpha}\right)^\beta} \quad (3)$$

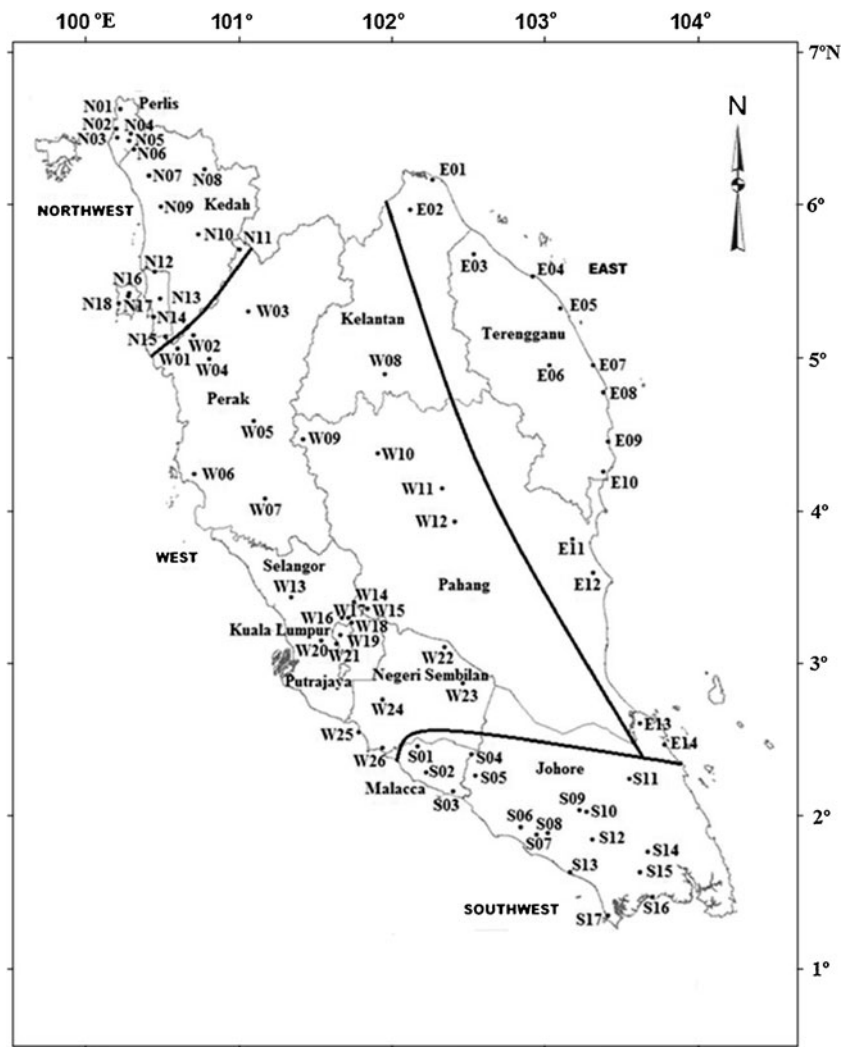
$$F(x; \alpha, \beta) = 1 - e^{-\left(\frac{x}{\alpha}\right)^\beta} \quad (4)$$

for $x > 0$ and $\alpha, \beta > 0$, where α is the shape parameter, and β is the scale parameter.

Lognormal distribution is a probability distribution of a random variable in which the logarithmic function is normally distributed in the probability theory. The PDF and CDF are written as:

$$f(x; \mu, \sigma) = \frac{1}{x\sigma\sqrt{2\pi}} e^{-\frac{(\ln x - \mu)^2}{2\sigma^2}} \quad (5)$$

Fig. 1 Study region and rain gauging stations



$$F(x; \mu, \sigma) = \frac{1}{2} \operatorname{erfc} \left[-\frac{\ln x - \mu}{\sigma\sqrt{2}} \right] \tag{6}$$

for $x > 0$, $\mu \in \mathbb{R}$ and $\sigma^2 > 0$ where $\operatorname{erfc}(x) = \frac{2}{\sqrt{\pi}} \int_x^\infty e^{-t^2} dt$ is the complementary error function, μ is the location parameter, and σ^2 is the squared scale parameter.

3.2 Parameter estimation

The parameter estimations in this study are interpreted using maximum likelihood estimation (MLE), since it is a commonly used statistical method in fitting a statistical model to data.

Suppose x is a continuous random variable with PDF $f(x; \theta_1, \theta_2, \dots, \theta_k)$, where $\theta_1, \theta_2, \dots, \theta_k$ are k unknown constant parameters which need to be estimated with an experiment conducted to obtain N independent observations, x_1, x_2, \dots, x_N . The estimation of parameters, $\hat{\theta}_1, \hat{\theta}_2, \dots, \hat{\theta}_k$, can be obtained by solving the differentiation of logarithmic likelihood function below:

$$\frac{d \sum_{i=1}^N \ln f(x_i; \theta_1, \theta_2, \dots, \theta_k)}{d\theta_j} = 0 \tag{7}$$

where $j=1, 2, \dots, k$

3.3 Goodness-of-fit tests

It is generally desirable to test the compatibility of a model and data by a statistical goodness-of-fit (GOF) test. GOF tests are used to describe the fitness of a distribution to a set of observations, and measures. GOF typically summarises the discrepancy between observed and expected values under the model in question. The best-fitted distribution will be chosen based on the minimum error produced. These errors may be measured by the following techniques.

Akaike Information Criterion (AIC) is derived by minimising the Kullback Leibler distance between the proposed model with the actual model. The formula of AIC is given as follows:

Table 1 List of stations

No.	Stations	Station Name	Latitude	Longitude
Northwest				
1	N01	Kaki Bukit	6°38'24"N	100°12'36"E
2	N02	Abi Kg. Bahru	6°30'36"N	100°10'48"E
3	N03	Padang Katong, Kangar	6°27'00"N	100°11'24"E
4	N04	Guar Nangka	6°28'48"N	100°16'48"E
5	N05	Arau	6°25'48"N	100°16'12"E
6	N06	Kodiang	6°22'12"N	100°18'00"E
7	N07	Alor Star	6°12'00"N	100°24'00"E
8	N08	Ampang Pedu	6°14'24"N	100°46'12"E
9	N09	Pendang	5°59'24"N	100°28'48"E
10	N10	SIK	5°48'36"N	100°43'48"E
11	N11	Dispensari Kroh	5°42'36"N	101°00'00"E
12	N12	Rumah Pam Bumbong Lima	5°33'36"N	100°26'24"E
13	N13	Bkt Berapit	5°22'48"N	100°28'48"E
14	N14	Ldg. Batu Kawan	5°15'36"N	100°25'48"E
15	N15	Rumah Penjaga JPS. Parit Nibong	5°07'48"N	100°30'36"E
16	N16	Klinik Bkt. Bendera	5°25'12"N	100°16'12"E
17	N17	Kolam Takungan Air Hitam	5°24'00"N	100°16'12"E
18	N18	Pintu A. Bagan, Air Itam	5°21'00"N	100°12'00"E
East				
19	E01	Kota Bharu	6°10'12"N	102°16'48"E
20	E02	To' Uban	5°58'12"N	102°08'24"E
21	E03	Sek. Keb. Kg. Jabi	5°40'48"N	102°33'36"E
22	E04	Kg. Merang, Setiu	5°31'48"N	102°57'00"E
23	E05	Stor JPS Kuala Terengganu	5°19'12"N	103°07'48"E
24	E06	Kg. Menerong	4°56'24"N	103°03'36"E
25	E07	Klinik Bidan, Jambu Bongkok	4°56'24"N	103°21'00"E
26	E08	Sek. Men. Sultan Omar, Dungun	4°45'36"N	103°25'12"E
27	E09	Sek. Keb. Kemasek	4°25'48"N	103°27'00"E
28	E10	JPS Kemaman	4°13'48"N	103°25'12"E
29	E11	Kuantan	3°46'48"N	103°13'12"E
30	E12	Rumah Pam Pahang Tua, Pekan	3°33'36"N	103°21'36"E
31	E13	Endau	2°35'24"N	103°40'12"E
32	E14	Mersing	2°27'00"N	103°49'48"E
Southwest				
33	S01	Jam. Sg. Simpangn, Jln. Empat	2°26'24"N	102°11'24"E
34	S02	Malacca	2°16'12"N	102°15'00"E
35	S03	Pekan Merlimau	2°09'00"N	102°25'48"E
36	S04	Ldg. Bkt. Asahan	2°23'24"N	102°33'00"E
37	S05	Tangkak	2°15'00"N	102°34'12"E
38	S06	Pintu Kawalan Separap Batu Pahat	1°55'12"N	102°52'48"E
39	S07	Sek. Men. Ingeris Batu Pahat	1°52'12"N	102°58'48"E
40	S08	Pintu Kawalan Sembrong	1°52'48"N	103°03'00"E
41	S09	Ldg. Kian Hoe, Kluang	2°01'48"N	103°16'12"E
42	S10	Kluang	2°01'12"N	103°19'12"E
43	S11	Ibu Bekalan Kahang, Kluang	2°13'48"N	103°36'00"E
44	S12	Ldg. Benut, Rengam	1°50'24"N	103°21'00"E
45	S13	Pintu Kawalan Tampok Batu Pahat	1°37'48"N	103°12'00"E
46	S14	Sek. Men. Bkt Besar di Kota Tinggi	1°45'36"N	103°43'12"E

Table 1 (continued)

No.	Stations	Station Name	Latitude	Longitude
47	S15	Senai	1°37'48"N	103°40'12"E
48	S16	Stor JPS Johor Bahru	1°28'12"N	103°45'00"E
49	S17	Ldg. Getah Kukup, Pontian	1°21'00"N	103°27'36"E
West				
50	W01	Rumah JPS, Alor Pongsu	5°03'00"N	100°35'24"E
51	W02	Selama	5°08'24"N	100°42'00"E
52	W03	Stn. Pemeriksaan Hutan, Lawin	5°18'00"N	101°03'36"E
53	W04	Pusat Kesihatan Bt. Kurau	4°58'48"N	100°48'00"E
54	W05	Ipoh	4°34'12"N	101°06'00"E
55	W06	Setiawan	4°13'12"N	100°42'00"E
56	W07	Rumah Kerajaan JPS, Chui Chak	4°03'00"N	101°10'12"E
57	W08	Gua Musang	4°52'48"N	101°58'12"E
58	W09	Ldg Boh	4°27'00"N	101°25'48"E
59	W10	S. K. Kg. Aur Gading	4°21'00"N	101°55'12"E
60	W11	Kg. Chebong	4°07'12"N	102°21'00"E
61	W12	Rumah Pam Paya Kangsar	3°54'00"N	102°25'48"E
62	W13	Ibu Bekalan Sg. Bernam	3°42'00"N	101°21'00"E
63	W14	Genting Sempah	3°22'12"N	101°46'12"E
64	W15	Janda Baik	3°19'48"N	101°51'36"E
65	W16	Kg. Sg. Tua	3°16'12"N	101°41'24"E
66	W17	Gombak	3°16'12"N	101°43'48"E
67	W18	Empangan Genting Kelang	3°14'24"N	101°45'00"E
68	W19	JPS. Wilayah Persekutuan	3°09'36"N	101°40'48"E
69	W20	Subang	3°07'12"N	101°33'00"E
70	W21	Petaling Jaya	3°06'00"N	101°39'00"E
71	W22	Sg. Lui Halt	3°04'48"N	102°22'12"E
72	W23	Ldg. Sg. Sabaling	2°51'00"N	102°29'24"E
73	W24	Stor JPS Sikamat Seremban	2°44'24"N	101°57'36"E
74	W25	Hospital Port Dickson	2°31'48"N	101°48'00"E
75	W26	Ldg. Sengkang	2°25'48"N	101°57'36"E

$$AIC = 2k - 2 \ln L \tag{8}$$

where k is the number of parameters in the statistical model, and L is the maximised value of the likelihood function for the estimated model.

The Kolmogorov–Smirnov (KS) test was used to determine the maximum difference between the hypothesised distribution with the empirical distribution. The KS test statistic is defined as:

$$D = \max_{1 \leq i \leq N} \left(\left| F(x_i) - \frac{i-1}{N} \right|, \left| \frac{i}{N} - F(x_i) \right| \right) \tag{9}$$

where x_i is the increasing ordered data, F is the theoretical cumulative distribution, and N is the sample size.

Anderson–Darling (AD) was applied to compare the model fitting between an observed CDF with an expected CDF. For AD tests, the definition is as follows:

$$A^2 = -n - \frac{1}{n} \sum_{i=1}^n (2i-1) [\ln F(X_i) + \ln(1 - F(X_{n+1-i}))] \tag{10}$$

where F is the CDF of the specified distribution and X_i are the ordered data.

3.4 Standardised Precipitation Index

The SPI was designed by McKee et al. (1993) to quantify the precipitation deficit on multiple time scales. For SPI calculation, a long-term precipitation record at the desired station is first fitted to a probability distribution which can be obtained by applying GOF tests and then transformed into a normal distribution where the mean SPI is zero (McKee et al. 1993). A positive SPI indicates that the observed precipitation is greater than the mean precipitation, while a negative SPI indicates the contrary. It is also reported that the SPI can be

used to monitor both dry and wet conditions (Morid et al. 2006).

The alternative method of SPI calculation with the precipitation data fitted to a gamma distribution for each time-scale can be expressed as a function involving the rainfall amount (x_i), the mean precipitation value (\bar{x}), and the standard deviation precipitation (s) (McKee et al. 1993; Sirdas and Sen 2001; Bacanli et al. 2008; Khan et al. 2008).

$$SPI = \frac{x_i - \bar{x}}{s} \quad (11)$$

The SPI application with the precipitation data fitted to a lognormal distribution can be simplified as the difference between logarithmic transformation of the dataset ($\ln(x)$), and the sample mean of the transformed data ($\hat{\mu}_y$) divided by the sample standard deviation ($\hat{\sigma}_y$) (Zhang et al. 2009).

$$SPI = \frac{\ln(x) - \hat{\mu}_y}{\hat{\sigma}_y} \quad (12)$$

The drought and wetness severity applied in this study is defined in Table 2. The sample mean and standard deviation that are used to normalise the probability distribution in determining the SPI values are based on the monsoon period, since the climate changes in Peninsular Malaysia are commonly affected by the monsoon season. Hence, the sample set is defined by the monsoon periods, specially the northeast monsoon (November–February), southwest monsoon (May–August) and inter-monsoon (March–April and September–October), in order to determine the sample mean and standard deviation for SPI computation.

3.5 Mann–Kendall trend test

The Mann–Kendall trend test (Mann 1945; Kendall 1975) is used to measure the trend for drought and wet events with respect to SPI, and is measured by the correlation between the ranks of observations and their time sequences (Hamed 2009).

Table 2 The standardised precipitation index (SPI) categories based on the initial classification of SPI values

Category	SPI
Extremely wet	2.00 and above
Severely wet	1.50 to 1.99
Moderately wet	1.00 to 1.49
Near normal	−0.99 to 0.99
Moderately dry	−1.00 to −1.49
Severely dry	−1.50 to −1.99
Extremely dry	−2.00 and less

For a time-series $\{x_i; t=1, 2, \dots, n\}$, the test statistic S is calculated as:

$$S = \sum_{i=1}^{n-1} \sum_{j=i+1}^n a_{ij} \quad (13)$$

where $a_{ij} = \text{sign} = (x_j - x_i) \begin{cases} 1 & ; x_i < x_j \\ 0 & ; x_i = x_j \\ -1 & ; x_i > x_j \end{cases}$ and n is the

sample size.

The value of mean and variance of S are calculated under the assumption that the data are independent and identically distributed as follows:

$$E(S) = 0 \quad (14)$$

$$V_0(S) = \frac{n(n-1)(2n+5)}{18} \quad (15)$$

The variance of S is reduced with the existence of tied ranks or equal observations in the data:

$$V_0^* = \frac{n(2n+5) - \sum_{j=1}^m t_j(t_j-1)(2t_j+5)}{18} \quad (16)$$

where m is the number of groups of tied ranks, each with t_j tied observations.

The standardised statistics (Z) for the one-tailed test are formulated as follows:

$$Z = \begin{cases} \frac{(S+1)}{\sqrt{V_0(S)}} & ; S > 0 \\ 0 & ; S = 0 \\ \frac{(S+1)}{\sqrt{V_0(S)}} & ; S < 0 \end{cases} \quad (17)$$

The null hypothesis of no trend is rejected if $|Z| > 1.96$ at the 5 % significance level.

3.6 Kriging method

Kriging is a geostatistical method which is applicable with the assumption of the distances or direction between sample points that reflect a spatial correlation that can be employed in explaining the variation in the surface. Kriging suits a mathematical function to a certain number of points which can be also fitted within a specified radius in determining the output value for the entire region. Kriging is a multistep process that involves an exploratory statistical analysis of the dataset, variogram modelling and surface creation. The weights of the kriging method rely on the distance between the measured points with the prediction location and overall spatial arrangement of the measured points.

Kriging analyses the measurement of values surrounded to define a prediction for the unmeasured region. Hence, the

trend pattern for the entire region of Peninsular Malaysia will be determined using the kriging method.

The general formula for the interpolator is recognised as a weighted sum of the data, which include the measured value at the i th location, $Z(s_i)$, an unknown weight for the measured value at the i th location, λ_i , the prediction location, s_0 , and the number of measured values, N .

$$\widehat{Z}(s_0) = \sum_{i=1}^N \lambda_i Z(s_i) \tag{18}$$

A general approach in solving with the kriging system equation is to apply the semivariogram function, $\Upsilon(h)$ (Merino et al. 2001). The estimation of semivariogram can be obtained based on the following equation:

$$\gamma(h) = \frac{1}{2n(h)} \sum_{i=1}^{n(h)} [Z(s_i) - Z(s_{i+h})]^2 \tag{19}$$

where $Z(s_i)$ and $Z(s_{i+h})$ are the measured values of Z at the point of i and $i+h$, respectively, with a separation distance h , and $n(h)$ is the number of pairs of sample points grouped with similar separation distance.

The semivariogram modelling is based on the fitting of parametric semivariogram models to the sample semivariogram models to ensure the unbiased results. The most common semivariogram models employed to describe the spatial variability of the variables are linear, spherical, exponential, and Gaussian models. The definition of the parameters (nugget, sill and range) for models characterization is illustrated in Fig. 2 and the expression of semivariogram models are described in Table 3.

3.6.1 Cross validation

Cross validation is an application used to compare the estimated kriged values obtained from various semivariogram models with the actual measured values. This method

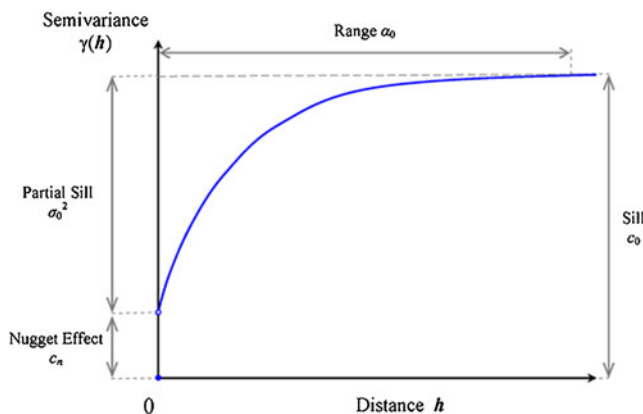


Fig. 2 Illustration of semivariance parameters

Table 3 Description of semivariogram models

Variogram model	Variogram, $\Upsilon(h)$
Linear	$\gamma(h) = \begin{cases} c_n + \sigma_0^2 h & , \text{ if } h > 0 \\ 0 & , \text{ otherwise} \end{cases}$
Spherical	$\gamma(h) = \begin{cases} c_0 & , \text{ if } h > a_0 \\ c_n + \sigma_0^2 \left[\frac{3h}{2a_0} - \frac{1}{2} \left(\frac{h}{a_0} \right)^3 \right] & , \text{ if } 0 < h \leq a_0 \\ 0 & , \text{ otherwise} \end{cases}$
Exponential	$\gamma(h) = \begin{cases} c_n + \sigma_0^2 \left[1 - \exp\left(-\frac{h}{a_0}\right) \right] & , h > 0 \\ 0 & , \text{ otherwise} \end{cases}$
Gaussian	$\gamma(h) = \begin{cases} c_n + \sigma_0^2 \left[1 - \exp\left(-\frac{h^2}{a_0^2}\right) \right] & , \text{ if } h > 0 \\ 0 & , \text{ otherwise} \end{cases}$

uses a quantification of errors based on the semivariogram models associated with kriging application. The predicted value for a selected station is obtained by discarding the corresponding measured value from the whole dataset temporarily and calculating the particular prediction result based on the remaining dataset using kriging method. The errors produced are analysed using five summary statistics as stated below.

Mean error (ME) is used to calculate the average different between the measured values and the predicted values. The best fitting model is chosen based on the ME values that are closer to 0. The expression of ME is as follows:

Table 4 Summary of parameter estimation for northwest region

Station	Gamma		Weibull		Lognormal	
	α	β	α	β	μ	σ
N01	0.5922	27.2020	16.3940	1.4305	2.3952	0.8573
N02	0.7603	18.2470	13.5330	1.1973	2.1243	1.0073
N03	0.7141	19.4260	13.0620	1.0659	2.0295	1.1401
N04	0.6533	20.4860	12.5140	1.0729	1.9904	1.1288
N05	0.7464	19.6700	13.9550	1.1010	2.1130	1.1087
N06	0.7070	19.3590	12.8840	1.0610	2.0133	1.1457
N07	0.7376	19.9540	13.9170	1.0766	2.0984	1.1313
N08	0.5935	24.3500	13.3720	1.0557	2.0479	1.1511
N09	0.5992	25.2330	13.6430	0.9932	2.0335	1.2157
N10	0.8803	19.2080	16.8380	1.2377	2.3584	0.9954
N11	0.7609	17.4770	12.7290	1.0842	2.0127	1.1246
N12	0.6722	24.4910	15.4530	1.0806	2.2052	1.1344
N13	0.6860	22.8150	14.9450	1.1267	2.1935	1.0822
N14	0.7715	20.2930	14.9800	1.0759	2.1737	1.1373
N15	0.9537	21.0540	20.3450	1.3032	2.5714	0.9548
N16	0.5595	31.6820	15.8990	0.9892	2.1842	1.2305
N17	0.5860	26.2730	13.9300	0.9991	2.0578	1.2106
N18	0.7549	25.7660	18.4340	1.0781	2.3803	1.1457

Table 5 Summary of parameter estimation for east region

Station	Gamma		Weibull		Lognormal	
	α	β	α	β	μ	σ
E01	0.3353	56.9890	15.7480	0.9610	2.1579	1.2517
E02	0.5298	36.1580	17.8580	1.1142	2.3658	1.1098
E03	0.5866	34.2050	19.1720	1.2405	2.4895	0.9918
E04	0.4505	51.5610	20.3250	1.0435	2.4604	1.1645
E05	0.3359	54.8810	15.0060	0.9437	2.0985	1.2681
E06	0.3885	49.0650	16.2920	0.9553	2.1877	1.2691
E07	0.4256	50.7400	19.8620	1.1526	2.4899	1.0658
E08	0.4093	43.6040	15.0550	0.9578	2.1108	1.2558
E09	0.4475	43.4120	17.0870	1.0364	2.2829	1.1780
E10	0.3698	49.6630	15.1970	0.9463	2.1127	1.2695
E11	0.4221	46.2630	16.7720	0.9795	2.2320	1.2375
E12	0.3704	51.1520	15.7860	0.9621	2.1608	1.2536
E13	0.4408	45.1200	17.0030	0.9810	2.2463	1.2358
E14	0.4085	43.8790	15.4370	0.9975	2.1596	1.2124

$$ME = \frac{\sum_{i=1}^n [\hat{Z}(s_i) - Z(s_i)]}{n} \tag{20}$$

Root mean square error (RMSE) is applied to indicate the accuracy of the certain model in predicting the measured values. Hence, the minimum error obtained will contribute to a more accurate model. The RMSE is defined as:

$$RMSE = \sqrt{\frac{\sum_{i=1}^n [\hat{Z}(s_i) - Z(s_i)]^2}{n}} \tag{21}$$

Average standard error (ASE) is the predicted standard error which describes the standard error related to the estimated results. The ASE is described as:

$$ASE = \sqrt{\frac{\sum_{i=1}^n \hat{\sigma}^2(s_i)}{n}} \tag{22}$$

Mean standardised error (MSE) is the standard error based on the mean prediction error over the prediction standard deviation. The MSE values should be closer to ASE values for a better model. The definition of MSE is shown as:

Table 7 Summary of parameter estimation for west region

Station	Gamma		Weibull		Lognormal	
	α	β	α	β	μ	σ
W01	0.7403	20.7860	14.5920	1.0809	2.1476	1.1327
W02	1.0502	18.5130	19.6630	1.206	2.5012	1.0375
W03	0.6828	18.0610	11.5900	1.0729	1.9136	1.1258
W04	0.8824	18.4830	15.8840	1.0934	2.2384	1.1282
W05	0.7834	20.2680	14.9760	1.0474	2.1565	1.1633
W06	0.6458	21.5100	12.7400	1.0247	1.9830	1.1732
W07	1.8193	13.1760	26.1170	1.3703	2.8423	0.9251
W08	0.6736	20.8070	12.9730	1.0313	2.0044	1.1740
W09	0.8826	12.6940	11.0670	1.1654	1.9096	1.0470
W10	1.1976	15.5070	19.3300	1.3640	2.5396	0.9193
W11	1.0155	18.1570	18.6130	1.2452	2.4619	1.0014
W12	0.6661	20.1580	12.6900	1.0913	2.0135	1.1164
W13	0.7582	21.0810	15.0130	1.0318	2.1507	1.1829
W14	0.3422	40.1970	12.6280	1.0491	1.9871	1.1560
W15	0.7816	15.5990	12.0580	1.2348	2.0234	0.9903
W16	0.7300	20.4990	13.9450	1.0186	2.0697	1.1916
W17	0.7613	20.0210	14.2880	1.0290	2.0996	1.1826
W18	0.7568	19.8750	14.1040	1.0268	2.0855	1.1842
W19	0.7279	21.5560	14.6280	1.0129	2.1144	1.2015
W20	0.7599	20.7400	14.8660	1.0529	2.1521	1.1587
W21	0.7840	22.1820	16.3560	1.0290	2.2348	1.1866
W22	1.2301	18.6670	24.0890	1.3067	2.7417	0.9671
W23	0.6770	21.4090	13.6950	1.1148	2.1009	1.0927
W24	0.7714	18.4000	13.5190	1.0756	2.0688	1.1350
W25	0.6749	23.4830	14.7350	1.0573	2.1458	1.1533
W26	0.4947	36.8350	16.3430	1.0456	2.2436	1.1680

Table 6 Summary of parameter estimation for southwest region

Station	Gamma		Weibull		Lognormal	
	α	β	α	β	μ	σ
S01	0.8512	18.1390	15.1340	1.1369	2.2105	1.0868
S02	0.6802	22.0010	13.8240	1.0184	2.0611	1.1881
S03	0.6521	23.7680	14.2810	1.0272	2.0986	1.1816
S04	0.9275	17.8330	16.4090	1.1694	2.3058	1.0615
S05	0.8036	17.7490	13.7610	1.1286	2.1118	1.0855
S06	0.9626	16.3990	15.9160	1.2217	2.2962	1.0207
S07	0.7732	20.7350	15.4320	1.1000	2.2130	1.1201
S08	0.7592	19.4710	14.4390	1.1920	2.1870	1.0322
S09	0.9807	21.2710	20.8160	1.1499	2.5356	1.0864
S10	0.5434	27.4620	13.5350	1.0374	2.0504	1.1662
S11	0.5133	33.0460	15.1880	1.0176	2.1546	1.1949
S12	0.8553	18.8070	15.8160	1.1512	2.2609	1.0734
S13	1.0852	21.0580	23.3720	1.2379	2.6868	1.0152
S14	0.5831	23.6630	12.6600	1.0528	1.9915	1.1491
S15	0.5985	25.5370	14.0450	1.0377	2.0874	1.1684
S16	0.6495	23.9170	14.3230	1.0236	2.0993	1.1879
S17	0.7123	23.4100	16.0810	1.1548	2.2791	1.0692

$$MSE = \frac{1}{n} \sum_{i=1}^n \frac{\widehat{Z}(s_i) - Z(s_i)}{\widehat{\sigma}(s_i)} \tag{23}$$

Root mean square standardised error (RMSSE) is the prediction standard errors where the result closer to 1 will be the better fit model. The variability in predictions are underestimated if RMSSE is greater than 1 and overestimated if RMSSE is smaller than 1. The interpretation of RMSSE is expressed as:

$$RMSSE = \sqrt{\frac{\sum_{i=1}^n \left\{ \left[\widehat{Z}(s_i) - Z(s_i) \right] / \widehat{\sigma}(s_i) \right\}^2}{n}} \tag{24}$$

where $\widehat{Z}(s_i)$ is the predicted value of variable Z at the point s_i , $Z(s_i)$ is the measured value at the point s_i , $\widehat{\sigma}^2(s_i)$ is the variance of estimated data, $\widehat{Z}(s_i)$, $\widehat{\sigma}(s_i)$ is the standard deviation of estimated data, $\widehat{Z}(s_i)$ and n is the number of measured values in the dataset.

4 Results and discussions

4.1 Parameter estimation

The parameters for each distribution are estimated using MLE and the results are summarised in Tables 4, 5, 6 and

7 based on the northwest, east, southwest and west regions, respectively. These parameters will be applied to GOF tests in order to determine the best fitting distribution for SPI computation.

4.2 Goodness-of-fit tests

The application of the three quantitative GOF tests discussed above state that the best-fitted distribution is selected based on the minimum error produced, which satisfies the corresponding criteria. Lognormal distribution was found to have the most minimum errors in all criteria of the GOF tests used in this study for the entire stations. Hence, the lognormal distribution is the most appropriate distribution to represent the daily rainfall amount in Peninsular Malaysia and the SPI calculation is based on the lognormal distribution. The summary of the GOF tests regarding to the northwest, east, southwest and west regions can be referred in Tables 8, 9, 10 and 11, respectively.

4.3 Application of Standardised Precipitation Index

The SPI calculation is based on the lognormal expression as the lognormal has been determined as the most appropriate distribution to represent the rainfall pattern. The SPI values obtained are classified into seven categories: extremely wet, severely wet, moderately wet, near normal, extremely dry, severely dry and moderately dry. The percentage of dry and

Table 8 Summary of GOF tests for northwest region

Stn	AIC			KS			AD		
	<i>G</i>	<i>W</i>	<i>L</i>	<i>G</i>	<i>W</i>	<i>L</i>	<i>G</i>	<i>W</i>	<i>L</i>
N01	28,773	28,498	26,760	0.299	0.177	0.117	374.42	132.10	52.01
N02	32,957	32,962	31,888	0.152	0.115	0.067	105.35	95.35	18.90
N03	32,863	32,775	32,170	0.129	0.078	0.052	60.65	61.58	19.81
N04	30,920	30,740	30,013	0.151	0.095	0.063	88.47	66.87	19.32
N05	32,419	32,391	31,738	0.115	0.094	0.045	60.19	67.75	13.95
N06	33,007	32,900	32,318	0.132	0.084	0.058	62.49	58.44	19.87
N07	33,036	32,986	32,391	0.117	0.075	0.043	54.59	62.13	18.23
N08	34,923	34,562	33,785	0.166	0.079	0.048	123.62	70.65	17.36
N09	36,375	36,096	35,402	0.159	0.098	0.062	95.49	73.34	25.66
N10	39,054	39,168	38,312	0.111	0.109	0.062	69.93	75.89	13.69
N11	36,897	36,831	36,269	0.120	0.081	0.058	55.86	57.29	24.24
N12	33,112	32,963	32,331	0.127	0.081	0.041	76.67	54.84	11.93
N13	35,329	35,164	34,334	0.140	0.116	0.083	103.97	74.59	23.28
N14	29,253	29,205	28,866	0.104	0.078	0.050	35.37	37.23	17.75
N15	28,776	28,907	28,323	0.092	0.079	0.032	45.37	40.87	3.88
N16	40,423	39,995	39,306	0.161	0.074	0.052	120.75	65.39	22.13
N17	36,720	36,384	35,692	0.163	0.081	0.055	103.96	68.58	26.09
N18	33,839	33,808	33,383	0.092	0.068	0.040	41.60	43.57	11.46

G Gamma, *W* Weibull, *L* Lognormal

Table 9 Summary of GOF tests for east region

Stn	AIC			KS			AD		
	<i>G</i>	<i>W</i>	<i>L</i>	<i>G</i>	<i>W</i>	<i>L</i>	<i>G</i>	<i>W</i>	<i>L</i>
E01	35,368	33,982	32,756	0.287	0.084	0.044	396.20	78.10	14.04
E02	37,688	37,079	36,109	0.175	0.069	0.033	224.01	45.00	6.84
E03	37,156	36,949	35,285	0.194	0.103	0.037	258.04	96.47	5.17
E04	32,842	32,246	31,120	0.229	0.094	0.055	225.14	73.76	8.56
E05	36,856	35,444	34,152	0.290	0.098	0.058	399.36	89.61	19.65
E06	50,383	48,798	47,651	0.247	0.083	0.050	403.75	78.88	27.20
E07	31,966	31,100	29,806	0.256	0.086	0.035	336.35	69.33	2.78
E08	36,044	35,126	34,077	0.239	0.091	0.055	257.62	81.72	18.57
E09	35,752	35,001	33,883	0.207	0.079	0.037	254.32	63.96	5.94
E10	38,141	36,931	35,747	0.264	0.083	0.054	336.33	82.21	18.41
E11	39,879	38,910	37,840	0.222	0.076	0.041	273.10	73.02	15.93
E12	36,134	34,989	33,837	0.260	0.085	0.046	327.95	74.06	13.52
E13	43,547	42,679	41,442	0.209	0.088	0.046	265.49	87.90	14.26
E14	38,820	37,762	36,546	0.239	0.084	0.040	314.25	76.54	14.71

G Gamma, *W* Weibull, *L* Lognormal

wet events for each category is then calculated with the following formula:

$$\text{Percentage} = \frac{m}{n} \times 100\% \quad (25)$$

where *m* is the number of days in each SPI category and *n* is the total number of days.

Table 12 shows the percentage of descriptive statistics of occurrences for dry and wet events with respect to each category. These results indicate that the average

percentages of events ranging from extremely wet to extremely dry are distributed near normal with a higher average in the extremely wet as compared with the extremely dry percentages. This is true, since Peninsular Malaysia is a region where rainfall is abundant and received throughout the year. Nevertheless, drought is also a phenomenon that needs attention in some parts of the region. During El Nino/Southern Oscillation, an event that happened between 1997 and 1998, Malaysia experienced low levels of rainfall that lead to drought

Table 10 Summary of GOF tests for southwest region

Stn	AIC			KS			AD		
	<i>G</i>	<i>W</i>	<i>L</i>	<i>G</i>	<i>W</i>	<i>L</i>	<i>G</i>	<i>W</i>	<i>L</i>
S01	37,574	37,590	37,174	0.087	0.075	0.062	41.65	44.07	20.62
S02	32,679	32,559	32,021	0.133	0.077	0.055	58.01	63.44	27.28
S03	31,627	31,468	30,902	0.138	0.092	0.054	68.12	63.18	21.23
S04	26,849	26,903	26,647	0.069	0.066	0.044	19.89	29.15	11.12
S05	32,403	32,427	31,825	0.104	0.082	0.044	48.79	59.84	12.20
S06	30,099	30,171	29,874	0.067	0.053	0.047	29.49	25.77	14.14
S07	34,802	34,749	34,319	0.102	0.070	0.048	45.32	40.54	17.85
S08	35,783	35,737	34,867	0.127	0.078	0.053	92.76	65.53	10.48
S09	24,935	24,974	24,923	0.049	0.050	0.053	8.09	15.44	15.57
S10	35,726	35,253	34,322	0.184	0.081	0.043	157.74	77.47	17.89
S11	41,958	41,315	40,319	0.185	0.091	0.051	196.30	76.43	18.75
S12	34,387	34,402	33,993	0.095	0.087	0.052	38.18	43.24	18.87
S13	27,574	27,645	27,581	0.037	0.050	0.066	9.03	13.15	16.95
S14	36,695	36,325	35,364	0.174	0.081	0.052	141.36	78.56	18.25
S15	40,260	41,009	39,041	0.159	0.076	0.049	125.65	80.51	25.03
S16	38,848	38,636	37,994	0.139	0.077	0.054	80.20	66.73	24.60
S17	37,501	37,371	36,577	0.120	0.072	0.038	99.50	51.32	9.05

G Gamma, *W* Weibull, *L* Lognormal

Table 11 Summary of GOF tests for west region

Stn	AIC			KS			AD		
	<i>G</i>	<i>W</i>	<i>L</i>	<i>G</i>	<i>W</i>	<i>L</i>	<i>G</i>	<i>W</i>	<i>L</i>
W01	39,029	38,965	38,333	0.113	0.081	0.049	61.06	62.96	18.25
W02	42,634	42,755	42,572	0.054	0.064	0.055	15.77	32.33	21.24
W03	32,411	32,271	31,525	0.150	0.090	0.060	82.12	72.09	21.28
W04	48,963	49,007	48,686	0.078	0.061	0.057	29.05	51.85	34.94
W05	39,624	39,625	39,105	0.100	0.078	0.048	44.20	70.57	27.89
W06	30,823	30,667	29,986	0.151	0.088	0.055	76.33	76.32	25.86
W07	40,934	40,861	41,603	0.047	0.030	0.095	19.34	6.56	81.32
W08	40,225	40,064	39,317	0.140	0.079	0.062	81.70	78.36	25.90
W09	44,607	44,686	43,892	0.107	0.085	0.061	59.55	80.63	27.24
W10	31,998	32,197	31,837	0.059	0.058	0.048	19.43	30.02	8.95
W11	26,602	26,711	26,395	0.071	0.083	0.038	21.14	34.43	6.69
W12	31,173	30,986	30,314	0.147	0.076	0.050	86.21	54.56	14.67
W13	40,168	40,128	39,675	0.105	0.080	0.052	43.54	62.20	29.00
W14	46,561	43,819	42,708	0.315	0.083	0.058	695.15	83.07	33.31
W15	35,859	35,849	34,763	0.143	0.094	0.058	112.06	77.52	14.02
W16	39,242	39,171	38,658	0.118	0.079	0.062	51.69	69.33	31.07
W17	39,125	39,097	38,614	0.108	0.080	0.056	44.84	66.57	28.64
W18	38,843	38,804	38,334	0.111	0.077	0.059	45.07	65.65	30.25
W19	40,815	40,730	40,280	0.115	0.074	0.058	48.59	63.76	33.16
W20	39,933	39,900	39,351	0.106	0.071	0.046	48.59	66.78	26.27
W21	42,250	42,242	41,817	0.093	0.071	0.047	39.57	66.02	33.84
W22	25,650	25,721	25,782	0.061	0.052	0.062	11.04	10.95	19.99
W23	29,351	29,237	28,475	0.137	0.091	0.054	86.49	66.53	11.08
W24	33,856	33,828	33,328	0.112	0.072	0.049	44.44	54.24	19.19
W25	31,420	31,305	30,694	0.129	0.090	0.050	67.32	59.93	14.66
W26	31,168	30,641	29,783	0.188	0.089	0.048	177.16	56.10	8.49

G Gamma, *W* Weibull, *L* Lognormal

conditions, with some regions suffering water disruptions from April to September 1998. Peninsular Malaysia also experienced a long dry spell in 2005 (NRE 2007). From the data, the total average percentage of wet events (EW, SW and MW) is 17.43 %, which is less than the total average percentage of dry events (ED, SD and MD), which is at 18.36 %. Therefore, the results clearly emphasise that the dry events are equally as evident and significant as the wet events, even though most of the regions receive rainfall all year round.

4.4 Cross validation of kriging interpolation

Tables 13 and 14 interpret the results of cross validation for kriging interpolation based on linear, spherical, exponential and Gaussian models. The best-fitted model is determined due to the near zero values of ME, smaller values of RMSE, closer values between ASE and MSE, and near 1 values of RMSSE. Based on the results, spherical semivariogram model is selected to describe the kriging interpolation for

Table 12 Percentages of wet and dry events according to the SPI categories

Category	Mean	Variance	Standard deviation	Coefficient of variation	Skewness	Kurtosis
EW	1.14	0.14	0.37	0.33	0.96	2.53
SW	4.91	0.24	0.49	0.10	-0.44	0.50
MW	11.38	0.86	0.93	0.08	-1.51	5.66
NN	64.22	2.64	1.63	0.03	2.48	11.15
MD	11.61	1.19	1.09	0.09	-0.71	1.73
SD	5.83	0.76	0.87	0.15	0.18	-0.27
ED	0.92	0.34	0.59	0.64	1.32	1.38

EW extremely wet, *SW* severely wet, *MW* moderately wet, *NN* near normal, *MD* moderately dry, *SD* severely dry, *ED* extremely dry

Table 13 Summary of cross validation with various models for dry events

Semivariogram model	ME	RMSE	ASE	MSE	RMSSE
Linear	-0.3065	6.7801	0.0963	-0.3676	8.1306
Spherical	0.0552	6.7133	0.2059	0.0310	3.7647
Exponential	-0.2071	6.7148	0.1035	-0.2309	7.4882
Gaussian	-0.2415	6.7378	0.1025	-0.2720	7.5886

both of the dry and wet events. Hence, the kriging prediction for trend test proceeded based on the spherical semivariogram model.

4.5 Trend test

Figure 3 shows the Z values for drought occurrences that have been categorised into moderately, severely and extremely dry as defined by the SPI. The darker colour represents the more positive trend while the lighter colour implies the more negative trend. It can be observed that the eastern and western regions of Peninsular Malaysia are dominated by increasing trends, the majority of which have values that are significant at a more than 95 % confidence level. Significantly, the northwest and southwest regions are occupied almost equally by both the increasing and decreasing trends at a more than 95 % confidence level, with a slight propensity toward downward trend domination. The results imply that a large part of eastern and western regions are expected to have lower precipitation during drought episodes and even drier dry events. The northwest and southwest regions, on the other hand, are expected to have more drought occurrences but not as severe as those in the eastern and western regions. Nevertheless, the drought occurrences in the northwest and southwest regions are still significant, since there are still stations that have significant upward trends.

Figure 4 shows the Z values for wet seasons that are summarised for moderately, severely and extremely wet conditions as defined by the SPI. The darker colour indicates the more positive trend while the lighter colour represents the more negative trend. Significantly, the results demonstrate that the northwest and southwest regions are characterised by decreasing trends at a more than 95 % confidence level, while the eastern and western regions are

Table 14 Summary of cross validation with various models for wet events

Semivariogram model	ME	RMSE	ASE	MSE	RMSSE
Linear	-0.0036	3.9475	0.0914	-0.0046	4.9897
Spherical	0.0405	3.9656	0.1162	0.0403	3.9394
Exponential	0.0012	3.9468	0.0915	0.0015	4.9820
Gaussian	0.0047	3.9451	0.0916	0.0059	4.9719

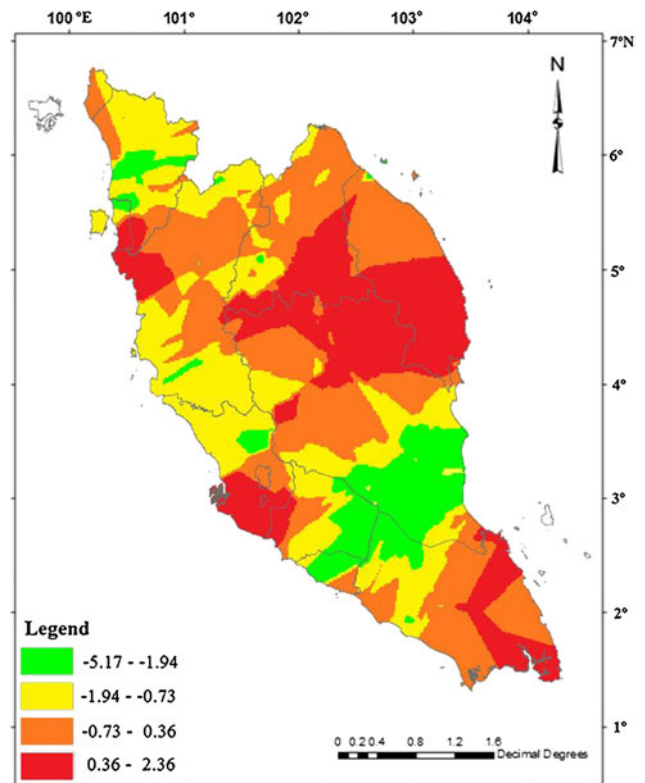


Fig. 3 Kriging displaying Z values for dry events

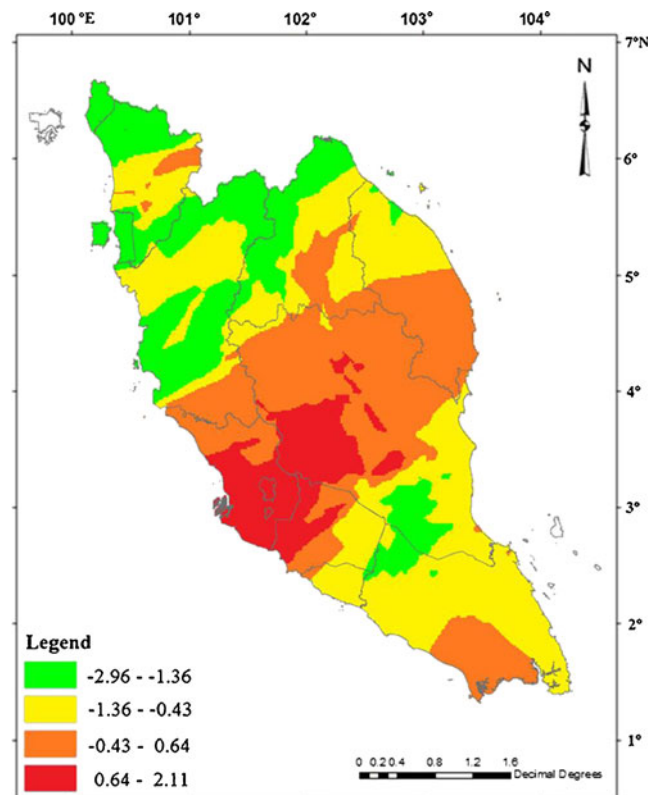


Fig. 4 Kriging displaying Z values for wet events

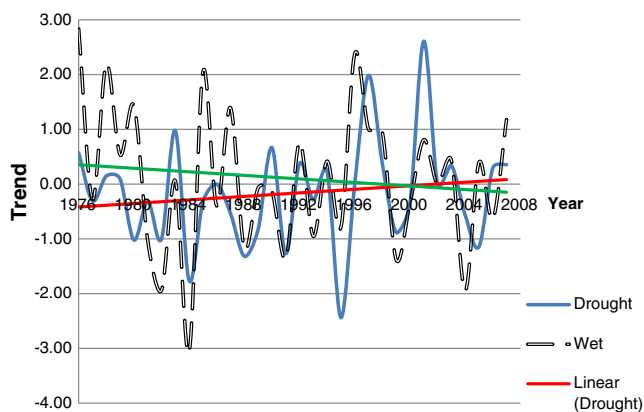


Fig. 5 The annual trend values for the northwest region

dominated by increasing trends at more than 95 % confidence level. This means that the east and west regions are expected to experience heavy rainfall during the wet periods, which may cause flooding at certain areas in the region. On the other hand, the northwest and southwest regions are expected to have a decrease in wet events.

In order to describe clearly the trends of dry and wet events in Peninsular Malaysia, the annual trend of a randomly selected station at each region is plotted to represent the trend behaviour for the corresponding region for further justification.

Figures 5, 6, 7 and 8 indicate the time-series plots for the annual trend of the northwest, east, southwest and west regions. The results imply an obvious increasing trend for the drought events and a significant decreasing trend for the wet events for northwest and southwest regions. The trends generally show a significant upward or positive trend for the drought events, which are predicted to increase with time and these regions are expected to receive less precipitation during these events. The wet event exhibits a decreasing trend that may be interpreted as having lesser rainfall amount during this event. Hence, the northwest and southwest regions are predicted to have a higher probability of drought occurrence during dry events and not much rain during wet events.

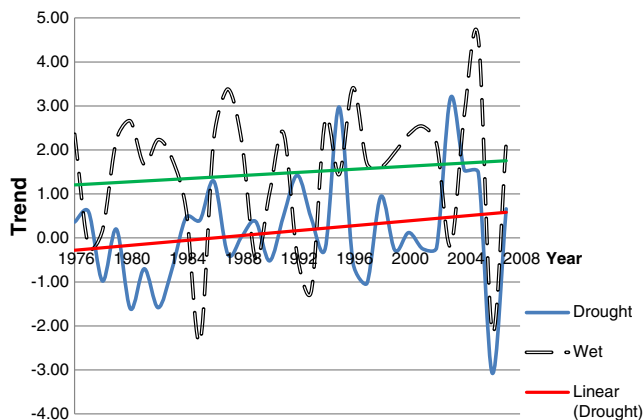


Fig. 6 The annual trend values for the east region

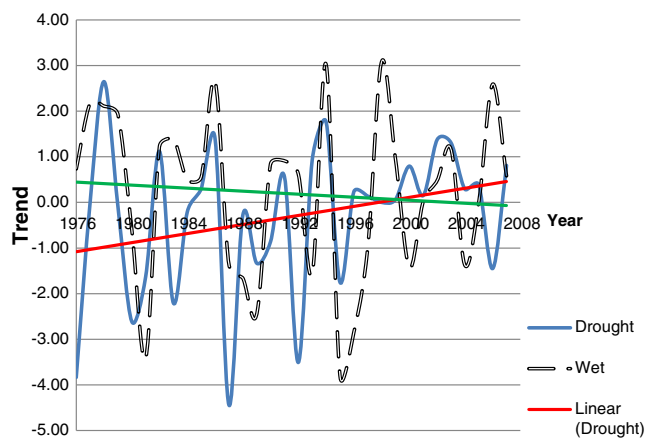


Fig. 7 The annual trend values for the southwest region

The time-series plots also indicate that the eastern and western regions are experiencing a significant increase in both dry and wet events. These results imply that the east and west regions are going through a high percentage of significant upward trends that may be translated into the expectation of receiving lower rainfall during drought episodes and heavy rainfall during the wet events.

Therefore, from the results of the annual trend, the eastern and western regions are expected to experience an upward trend during the drought events and also an increasing trend during the wet events. However, for regions that are going through a downward trend, there is also the potential for either drought or flood threats in those regions, as these two extreme events are expected to happen anywhere in Malaysia.

5 Conclusions

The categorisation of rainfall events is important in order to predict and thus prevent meteorological disasters. Based on the fitting distribution, lognormal distribution is recognised as the best-fitted distribution to represent the daily rainfall in Peninsular Malaysia. The SPI results suggest that there is a

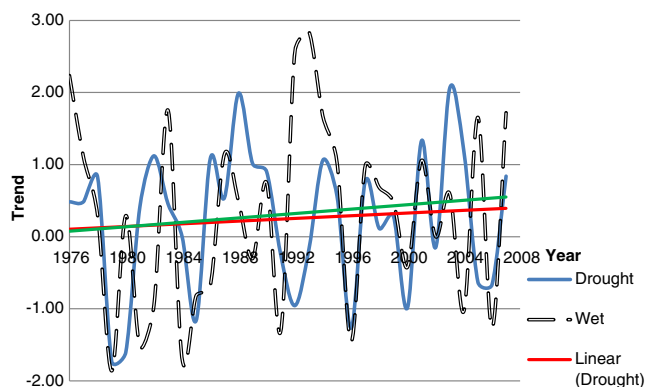


Fig. 8 The annual trend values for the west region

significant upward trend in daily precipitation, especially for the east and west regions during drought episodes. On the other hand, for the wet events, the SPI showed a significant downward trend, except in the eastern and western parts. The drought occurrences experienced a statistically significant upward trend, with the possibility of the existence of an increasing pattern. This indicates that less precipitation is received during the dry events (that affects most of Peninsular Malaysia), and more precipitation is received during the wet events (in certain areas), with these patterns expected to increase over time. The time-series plots confirm that the whole Peninsular Malaysia is predicted to have an increasing trend during drought events while the majority of its regions are expected to experience a decreasing trend for the wet events, except in east and west parts. These results suggest that certain regions in Peninsular Malaysia are going through drier dry events and wetter wet events, especially the eastern and western regions. These would increase the possibilities of having drought and flood events in Malaysia. Although these two events cannot be prevented and may negatively affect society, the loss can be reduced through mitigation and planning. The results of this study could offer some information on the regions that require attention because these disasters illustrate the vulnerability of economic, social, political and environmental systems to a variable climate.

Acknowledgments The authors are grateful to the Malaysian Meteorological Department and Malaysian Drainage and Irrigation Department for providing the daily precipitation data. The work is financed by the MyPhD Scholarship, provided by the Ministry of Higher Education of Malaysia and Universiti Teknologi Malaysia.

References

- Bacanli UG, Dikbas F, Baran T (2008) Drought analysis and a sample study of Aegean Region. Sixth International Conference on Ethics and Environmental Policies, Padova, 23–25 October

- Bordi I, Fraedrich K, Sutera A (2009) Observed drought and wetness trends in Europe: an update. *Hydrol Earth Syst Sci* 13:1519–1530
- Deni SM, Suhaila J, Zin WZW, Jemain AA (2009) Trends of wet spells over Peninsular Malaysia during monsoon seasons. *Sains Malaysiana* 38(2):133–142
- Department of Defense (2011) Trends and implications of climate change for national and international security. Office of the Under Secretary of Defense, Washington
- Hamed KH (2009) Exact distribution of the Mann–Kendall trend test statistic for persistent data. *J Hydrol* 365:86–94
- Kendall MG (1975) Rank correlation methods. Griffin, London
- Khan S, Gabriel HF, Rana T (2008) Standard precipitation index to track drought and assess impact of rainfall on watertables in irrigation areas. *Irrig Drain Syst* 22:159–177
- Mann HB (1945) Nonparametric tests against trend. *Econometrica* 13:245–259
- McKee TB, Doesken NJ, Kleist J (1993) The relationship of drought frequency and duration on time scale. Preprints, Eighth Conf on Applied Climatology, Anaheim, CA. Am Meteor Soc, Boston pp. 179–184
- Merino GG, Jones D, Stooksbury DE, Hubbard KG (2001) Determination of semivariogram models to krige hourly and daily solar irradiance in Western Nebraska. *J Appl Meteorol* 40: 1085–1094
- Ministry of Natural Resources & Environment (NRE) (2007) Flood and drought management in Malaysia. Deraf Teks Ucapan Jabatan Pengairan & Saliran Malaysia
- Morid S, Smakhtin V, Moghaddasi M (2006) Comparison of seven meteorological indices for drought monitoring in Iran. *Int J Climatol* 26:971–985
- Sirdas S, Sen Z (2001) Application of the standardized precipitation index (SPI) to the Marmara Region, Turkey. *Integrated Water Resources Management*. IAHS Publ. no. 272.2001
- Sonmez FK, Komusu AU, Erkan A, Turgu E (2005) An analysis of spatial and temporal dimension of drought vulnerability in Turkey using the standardized precipitation index. *Nat Hazards* 35:243–264
- Suhaila J, Jemain AA (2009) Investigating the impacts of adjoining wet days on the distribution of daily rainfall amounts in Peninsular Malaysia. *J Hydrol* 368:17–25
- Yusof F, Hui-Mean F (2012) Use of statistical distribution for drought analysis. *Appl Math Sci* 6(21):1031–1051
- Zhang Q, Xu CY, Zhang Z (2009) Observed changes of drought/wetness episodes in the Pearl River Basin, China, using the standardized precipitation index and aridity index. *Theor Appl Climatol* 98:89–99